

Weakly nonlinear theory of grain boundary motion in patterns with crystalline symmetry

Denis Boyer

*Instituto de Física, Universidad Nacional Autónoma de México, Apartado Postal 20-364, 01000
México D.F., México*

Jorge Viñals

*Laboratory of Computational Genomics, Donald Danforth Plant Science Center, 975 North
Warson Rd, St. Louis, Missouri 63132.*

(November 21, 2018)

Abstract

We study the motion of a grain boundary separating two otherwise stationary domains of hexagonal symmetry. Starting from an order parameter equation appropriate for hexagonal patterns, a multiple scale analysis leads to an analytical equation of motion for the boundary that shares many properties with that of a crystalline solid. We find that defect motion is generically opposed by a pinning force that arises from non-adiabatic corrections to the standard amplitude equation. The magnitude of this force depends sharply on the misorientation angle between adjacent domains so that the most easily pinned grain boundaries are those with an angle $4^\circ \leq \theta \leq 8^\circ$. Although pinning effects may be small, they do not vanish asymptotically near the onset of this subcritical bifurcation, and can be orders of magnitude larger than those present in smectic phases that bifurcate supercritically.

The microstructure of a condensed phase and the distribution of topological defects largely determine its mechanical and thermodynamical response, as well as the temporal evolution of its non-equilibrium configurations. Continuum or hydrodynamic approaches to phases with broken symmetry are now well understood [1,2], including the long wavelength description of topological defects [3,4]. Nevertheless, a quantitative theory of defect motion (e.g., dislocation glide) remains a difficult problem because it requires short scale phenomena that lie beyond a hydrodynamic theory, and therefore beyond the degree of universality that such a description entails.

Bifurcations to states with broken symmetry are also encountered in a variety of physical, chemical and biological systems driven outside of thermodynamic equilibrium. The characteristic length scales involved are much larger than atomic dimensions, therefore making the observation and study of defects substantially easier. Here, amplitude or phase equations that focus on slow modulations of a base periodic pattern play the role of the hydrodynamic description [5]. It has been noted, for example, that at leading order hexagonal patterns are the dissipative analogues of a two dimensional, isotropic solid [6]. We focus in this paper on grain boundary motion in hexagonal patterns, and find many qualitative and quantitative similarities with grain boundary motion in crystalline solids. In contrast with the latter case, our starting model allows a detailed analysis of the breakdown of the long wavelength description of defect motion through an explicit multiple scale analysis. We are then able to derive analytically several results that are known only qualitatively or empirically in crystalline solids.

Hexagonal patterns formed in a spatially extended system (like in Langmuir monolayers [7] or block copolymer melts [8]) are often fairly disordered. They consist of randomly oriented grains separated by grain boundaries (arrays of dislocations in the low angle case), and are equivalent by symmetry to a polycrystalline solid. This nonequilibrium microstructure usually evolves on a very slow, fluctuation-dependent time scale due to pinning forces to defect motion. Our focus here is on a coarse grained model of a hexagonal pattern, and, in particular, on the motion of a grain boundary separating two domains with arbitrary

mis-orientation. We extend to this case a recent study of defect motion and pinning near a supercritical bifurcation involving stripe patterns (or smectic phases) [9]. We show that the coupling between the slow variables of an envelope description of the defect and the underlying (fast) periodicity of the base pattern leads to an effective periodic potential, the close analogue of the Peierls barrier acting on defects in a crystalline solid [10]. Furthermore, we find that the magnitude of the potential barrier does not vanish as the subcritical bifurcation point is approached, contrary to the case of smectic phases [9]. Hence, not only crystalline phases emerging from a subcritical bifurcation are harder than smectics in terms of the forces acting on topological defects, but also an envelope description that ignores the internal degrees of freedom of defects does not appear to be valid even near the bifurcation point. The self-generated pinning effects discussed here are expected to be a general feature of modulated phases, and can explain, for example, many grain boundary conformations that have been observed experimentally and numerically in block copolymer melts [11].

We study here the Swift-Hohenberg model of Rayleigh-Bénard convection with an additional quadratic term to allow the formation of hexagonal patterns [5,6],

$$\frac{\partial \psi}{\partial t} = \epsilon \psi - \frac{1}{k_0^4} (k_0^2 + \nabla^2)^2 \psi + g_2 \psi^2 - \psi^3. \quad (1)$$

The order parameter $\psi(\vec{x}, t)$ is related to the vertical velocity at the mid plane of the convective cell, ϵ is the reduced Rayleigh number, and g_2 can be related to deviations from Boussinesq behavior in the working fluid. The uniform solution $\psi = 0$ becomes unstable for $\epsilon > 0$ to a periodic pattern of wavelength $\lambda_0 = 2\pi/k_0$. Hexagonal patterns are stable for $-|\epsilon_m(g_2)| < \epsilon < \epsilon_M(g_2)$, and roll patterns for $\epsilon > \epsilon_M$. In this study, we chose $\epsilon \in [0, \epsilon_M]$ so that only hexagonal patterns are stable.

An approximate stationary solution for a configuration containing a planar grain boundary between two uniform and symmetric domains of hexagons that have a relative misorientation angle θ ($0 \leq \theta \leq \pi/3$, see Fig. 1) can be found by assuming that $\psi_0 = \sum_{n=1}^6 A_n e^{i\vec{k}_n \cdot \vec{x}} + c.c.$, where $A_n(x)$ are slowly varying envelopes, and x is the coordinate normal to the boundary. As $x \rightarrow -\infty$, $A_{1,2,3} \rightarrow A_0 = (g_2 + \sqrt{g_2^2 + 15\epsilon})/15$ exponentially

fast outside a boundary layer of thickness ξ [$A_n(x) = f_n(x/\xi)$], whereas $A_{4,5,6} \rightarrow 0$. As $x \rightarrow \infty$, $A_{4,5,6} \rightarrow A_0$ and $A_{1,2,3} \rightarrow 0$. We chose $|\vec{k}_n| = k_0$, $\vec{k}_{1,4} = k_0(\cos(\phi)\hat{x} \mp \sin(\phi)\hat{y})$, where $\phi = \pi/6 - \theta/2$, and the other vectors \vec{k}_n are obtained from these by rotations of $\pm 2\pi/3$ as indicated in Figure 1. In analogy with crystalline solids, a small angle grain boundary is well described as an array of penta-hepta defects (the dislocations cores of a hexagonal pattern), separated on average by a distance of the order λ_0/θ . However, since the projections of $\vec{k}_{1,2,3}$ on the x axis are usually not commensurate, the patterns observed along the boundary are not periodic.

We next focus on grain boundary motion and extend our earlier results for stripe patterns [9]. The amplitude equation formalism has already been used to study defect dynamics in hexagonal patterns [12]. Amplitude equations are obtained from a standard multiscale analysis of Eq. (1). For example, the equation for A_1 follows from the solvability condition

$$\int_x^{x+l_x} \frac{dx'}{l_x} \lim_{l_y \rightarrow \infty} \int_0^{l_y} \frac{dy'}{l_y} [L(\psi_0) + g_2\psi_0^2 - \psi_0^3] e^{-i\vec{k}_1 \cdot \vec{x}'} = 0, \quad (2)$$

where L is a linear operator that follows from Eq. (1) [13] and l_x a length of $O(\lambda_0)$ to be specified later. When both ϵ and $g_2 \rightarrow 0$, the length scale of variation of the A_n 's (*i.e.* the grain boundary thickness ξ) is much larger than λ_0 , and only non oscillatory terms contribute to the integral (2). The solvability condition leads to the usual amplitude equations that show that defects are either immobile or move with constant velocity [6].

If, on the other hand, ϵ and g_2 are small but finite, then the amplitudes are not strictly constant within a period l_x . Any oscillatory term in (2) of wavevector \vec{K} parallel to the normal x -axis does not integrate to zero, and the equation for the slowly varying amplitudes cannot be decoupled from the phase of the defect (yielding “non-adiabatic corrections” [14–16,5]). Although these contributions are small (non-analytic in both ϵ and g_2), they may have dramatic effects. In the case of Eq. (1), non-vanishing terms can arise from the cubic nonlinearity, and are proportional to $A_1^2 A_4$, $\bar{A}_1 \bar{A}_4^2$, $A_1 A_3 A_5$, $A_1 \bar{A}_3 \bar{A}_5$, $A_1 A_2 A_6$ and $A_1 \bar{A}_2 \bar{A}_6$. An oscillatory term proportional to $\cos(Kx')$ in Eq. (2) contributes to order $\exp(-|K\xi|)$ to the law of grain boundary of motion (see Eqs. (6) and (7) below). This contribution

is simplest when both $\epsilon \ll 1$ and $g_2 \ll 1$ so that $\xi \gg \lambda_0$ and a single mode with lowest K dominates. In this limit, the slowest non-adiabatic corrections are those proportional to $A_1 A_2 A_6$ and $A_1 \bar{A}_2 \bar{A}_6$, which have $K = |\vec{k}_2 + \vec{k}_6| = 2k_0 \sin(\theta/2)$ (see Fig. 1). The solvability condition (2) now reads

$$\begin{aligned} \frac{\partial A_1}{\partial t} = & -\frac{\partial F}{\partial \bar{A}_1} \\ & - \int_{x_0}^{x_0+l_x} \frac{dx}{l_x} 6A_1 \left(A_2 A_6 e^{-2ik_0 x \sin(\theta/2)} + \text{c.c.} \right), \end{aligned} \quad (3)$$

where $l_x = \lambda_0/[2 \sin(\theta/2)]$. The first two terms in Eq. (3) represent the standard amplitude equation with the Lyapunov functional

$$\begin{aligned} F = \int d\vec{r} \left[& -\epsilon \sum_{n=1}^6 |A_n|^2 + \frac{4}{k_0^2} \sum_{n=1}^6 |D_n A_n|^2 \right. \\ & - 2g_2 (\bar{A}_1 \bar{A}_2 \bar{A}_3 + \bar{A}_4 \bar{A}_5 \bar{A}_6 + A_1 A_2 A_3 + A_4 A_5 A_6) \\ & \left. + \frac{3}{2} \sum_{n=1}^6 |A_n|^4 + 3 \sum_{n<m} |A_n|^2 |A_m|^2 \right], \end{aligned} \quad (4)$$

with $D_n = \partial/\partial x_n$ the derivative along \vec{k}_n . Equations similar to (3) can be derived for the remaining amplitudes A_n (not shown). The last term in the r.h.s. of Eq. (3) is new and represents the dominant non-adiabatic correction in the limits $\epsilon \ll 1$ and $g_2 \ll 1$.

In order to derive an equation of motion for the grain boundary from the equations for the A_n , we first denote by $a_n(x)$ ($1 \leq n \leq 6$) the leading order amplitudes of the stationary grain boundary, solutions of the one-dimensional coupled Ginzburg-Landau equations $\partial F/\partial \bar{a}_n = 0$. We then look for solutions of the form $A_n(x, t) = a_n(x - x_{gb}(t))$, where $x_{gb}(t)$ is the now time-dependent position of the grain boundary [9]. We find,

$$D \dot{x}_{gb} = -p_{\text{hex}} \sin[2k_0 x_{gb} \sin(\theta/2)], \quad (5)$$

where $D = \int_{-\infty}^{\infty} dx \sum_{n=1}^6 (\partial_x a_n)^2$ is a friction coefficient, and

$$\begin{aligned} p_{\text{hex}} = \text{Max}_{\beta} \int_{-\infty}^{\infty} dx \cos [2k_0 \sin(2\theta)x + \beta] \{ & 3 [a_2 \partial_x (a_2^2 a_6) \\ & + a_6 \partial_x (a_6^2 a_2)] + 12 [a_1 \partial_x (a_1 a_2 a_6) + a_3 \partial_x (a_3 a_2 a_6) \\ & + a_4 \partial_x (a_4 a_2 a_6) + a_5 \partial_x (a_5 a_2 a_6)] \} \end{aligned} \quad (6)$$

is the (dimensionless) amplitude of a pinning force of wavelength $\lambda_0/[2 \sin(\theta/2)]$. This periodic force explicitly arises from the coupling between the slowly varying wave amplitudes and the periodicity of the base state in the integral term of Eq. (3). Equations (5) and (6) show that a planar grain boundary initially located at an arbitrary position relaxes toward the nearest minimum of the periodic pinning potential. The stationary and stable positions of the boundary are thus discrete, separated from each other by a distance $\Delta x_{gb} = \lambda_0/[2 \sin(\theta/2)] > \lambda_0$. The two wavevectors with the smallest projection on the grain boundary normal (\vec{k}_2 and \vec{k}_6 , see Figure 1) set the wavevector ($\vec{k}_2 + \vec{k}_6$) of the periodic pinning potential. The usual amplitude equation formalism would instead predict that $p_{\text{hex}} = 0$, and x_{gb} is arbitrary and decoupled from the phase of the pattern. Figure 1 shows three successive stable locations of the the grain boundary obtained by numerically solving Eq. (1). The values of Δx_{gb} determined numerically agree very well with the analytic result.

We expect equations of the form of Eq. (5) to be generic at a bifurcation, and not limited to hexagon-hexagon grain boundaries. In particular, we anticipate that non-adiabatic effects are important in block copolymer melts, and can explain the conformations of planar interfaces observed in these systems [11].

Remarkably, the present result for a pattern of hexagonal symmetry is analogous to the Peierls force acting on dislocations in crystalline solids [10]. Peierls calculated the energy of a single dislocation by summing over the interactions between atoms within two neighboring layers, their displacements given by continuous elasticity as a first approximation. The energy of the dislocation oscillates as a function of its position so that it can glide only if a force of finite amplitude acts on it (the Peierls' force). Here, we find that a similar force acts on assemblies of dislocations organized in arrays. Like in the simpler geometry studied by Peierls, the amplitude of the pinning force decays exponentially with the spatial thickness of the defect ξ . From Eq. (6), we find

$$p_{\text{hex}} \sim c^* A_0^4 e^{-2k_0 \sin(\theta/2)\xi a^*}, \quad (7)$$

with c^* and a^* dimensionless constants of order unity that can *a priori* depend on the

mis-orientation θ . At this point, we note an important distinction between defect motion in hexagonal patterns that emerge at a subcritical bifurcation, and in stripe patterns that bifurcate supercritically. The supercritical case was discussed in ref. [9] for a 90° boundary separating two domains of stripes given by Eq. (1) with $g_2 = 0$. The corresponding pinning force acting on the boundary, p_{stripe} , satisfies a relation similar to Eq. (7), with $\xi \sim 1/\sqrt{\epsilon}$. Hence $p_{\text{stripe}} \sim \exp(-1/\sqrt{\epsilon}) \rightarrow 0$, as the control parameter $\epsilon \rightarrow 0$. In the hexagonal phase, however, $\xi(\epsilon = 0) \simeq 15\lambda_0/(8\sqrt{6}\pi g_2)$ is finite. Therefore p_{hex} , although small, does not vanish when $\epsilon \rightarrow 0$ (nor when $\epsilon \rightarrow -|\epsilon_m(g_2)|$).

Figure 2 shows typical variations of the pinning force as a function of ϵ for different values of g_2 ($\theta = \pi/9$). The curves are given by Eq. (6), where the amplitudes a_n have been obtained by numerically integrating the system of equations $\partial F/\partial \bar{a}_n = 0$. For a value of g_2 as small as 0.3, p_{hex} is many orders of magnitude larger than p_{stripe} . Therefore, non-adiabatic effects in hexagonal, “crystalline-like”, patterns are difficult to avoid. Defects need to overcome much higher activation barriers, and will be much less easily un-pinned either upon the application of external stresses or random noise (that would be represented by additional terms in the r.h.s. of Eq. (5)).

Finally we study the dependence of the pinning force with grain boundary mis-orientation θ . Figure 3 displays $p_{\text{hex}}(\theta)$ for different values of the parameters g_2 and ϵ . We find that the least mobile grain boundaries, *i.e.* those for which the amplitude of the pinning force is maximal, have a low angle θ_M , typically such that $4^\circ \leq \theta_M \leq 8^\circ$. Both θ_M and the overall shape of $p_{\text{hex}}(\theta)$ depend weakly on g_2 and ϵ . Figure 3 also shows the pinning force vs. θ obtained from a direct numerical solution of Eq. (1) with $g_2 = 0.3$ and $\epsilon = 0.05$. Here p_{hex} is estimated by fitting grain boundary relaxation trajectories to Eq. (5), with the friction coefficient D assumed to be given by the analytic result. The numerical results compare reasonably well with the theory given the numerical difficulties in tracking the relaxation of the grain boundary in a finite sized system. Although the maximum value is lower and the curve flatter in the numerical case, the right order of magnitude is obtained, as well as a similar range for θ_M . The discrepancy can also be attributed in part to non-adiabatic

corrections of higher order to Eq. (6), that may not be negligible at $g_2 \sim 0.3$.

Our present analysis can qualitatively explain the properties of polycrystalline, partially ordered configurations that are typically observed at long times in many pattern forming systems with this symmetry [7,8]. Although the evolution defined by Eq. (1) is driven by the minimization of a Lyapunov functional, we expect that grain boundaries (and other topological defects) will become pinned at long times as the driving force for microstructure coarsening decreases. Therefore, the system will eventually reach metastable, glassy-like configurations that can only order by slow activated processes (presumably logarithmic in time, as already observed in [8] with a random forcing term added to Eq. (1)). We additionally note that defects observed in cold metals are essentially low angle grain boundaries in the range 5° and 10° [17], a value that compares very well with the values obtained by the present theory.

In summary, we have analyzed the motion of grain boundaries in hexagonal patterns from an order parameter equation and extended the standard Ginzburg-Landau equation for the slowly varying amplitude to incorporate non-analytic corrections. Like in crystalline phases, defect motion is opposed by short range forces with periodicity and amplitude that strongly depend on the mis-orientation angle between domains. Although small, these pinning forces can not be neglected asymptotically at long times in a coarsening system, even near onset, and are orders of magnitude higher than those produced in patterns of smectic symmetry.

We are indebted to François Drolet for useful discussions. This research has been supported by the U.S. Department of Energy, contract No. DE-FG05-95ER14566.

REFERENCES

- [1] P. Martin, O. Parodi, and P. Pershan, *Phys. Rev. A* **6**, 2401 (1972).
- [2] P. Chaikin and T. Lubensky, *Principles of condensed matter physics* (Cambridge University Press, New York, 1995).
- [3] A. Kosevich, in *Dislocations in Solids*, edited by F. Nabarro (North-Holland, New York, 1979), Vol. 1, p. 33.
- [4] D.R. Nelson and B.I. Halperin, *Phys. Rev. B* **19**, 2457 (1979); A.P. Young, *Phys. Rev. B* **19**, 1855 (1979).
- [5] M.C. Cross and P.C. Hohenberg, *Rev. Mod. Phys.* **65**, 851 (1993).
- [6] D. Walgraef, *Spatio-Temporal Pattern Formation* (Springer Verlag, New York, 1996).
- [7] C. Sagui and R.C. Desai, *Phys. Rev. E* **49**, 2225 (1994).
- [8] K.R. Elder, M. Katakowski, M. Haataja, and M. Grant, cond-mat/0107381.
- [9] D. Boyer and J. Viñals, cond-mat/0110254.
- [10] R. Peierls, *Proc. Phys. Soc. London* **52**, 34 (1940).
- [11] R.R. Netz, D. Andelman, and M. Schick, *Phys. Rev. Lett.* **79**, 1058 (1997), and references therein.
- [12] L. Tsimring, *Physica D* **89**, 368 (1996).
- [13] P. Manneville, *Dissipative Structures and Weak Turbulence* (Academic, New York, 1990).
- [14] Y. Pomeau, *Physica D* **23**, 3 (1986).
- [15] D. Bensimon, B.I. Shraiman, and V. Croquette, *Phys. Rev. A* **38**, 5461 (1988).
- [16] B.A. Malomed, A.A. Nepomnyashchy, and M.I. Tribelsky, *Phys. Rev. A* **42**, 7244 (1990).

[17] D. Hull and D.J. Bacon, *Introduction to Dislocations* (Pergamon Press, New York, 1992).

FIGURES

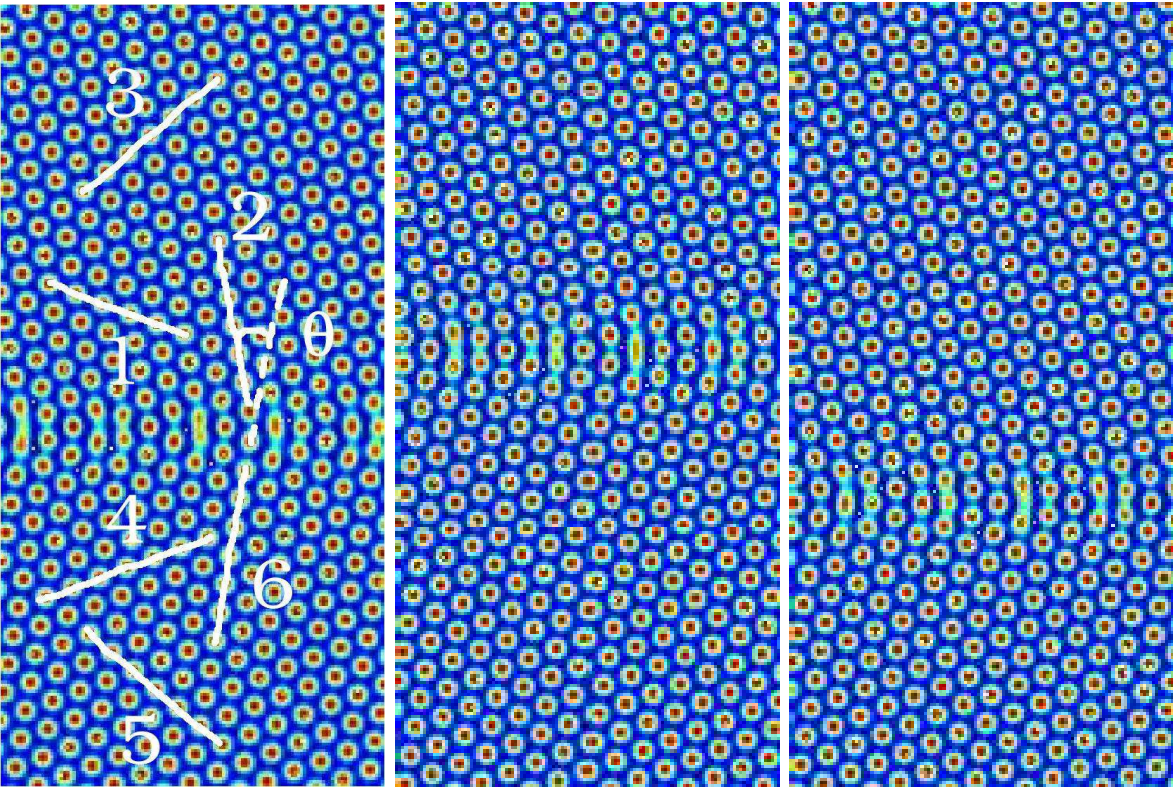


FIG. 1. Order parameter ψ in gray scale. Only a portion of a square grid of 512^2 points is shown with spacing $\Delta x = \sqrt{3}/2$ and $\lambda_0 = 8\Delta x$. Three locations are shown in which a planar grain boundary is stationary. The two hexagonal domains are defined by the sets $\{\vec{k}_1, \vec{k}_2, \vec{k}_3\}$ and $\{\vec{k}_4, \vec{k}_5, \vec{k}_6\}$ respectively, with a mis-orientation angle $\theta = \pi/9$.

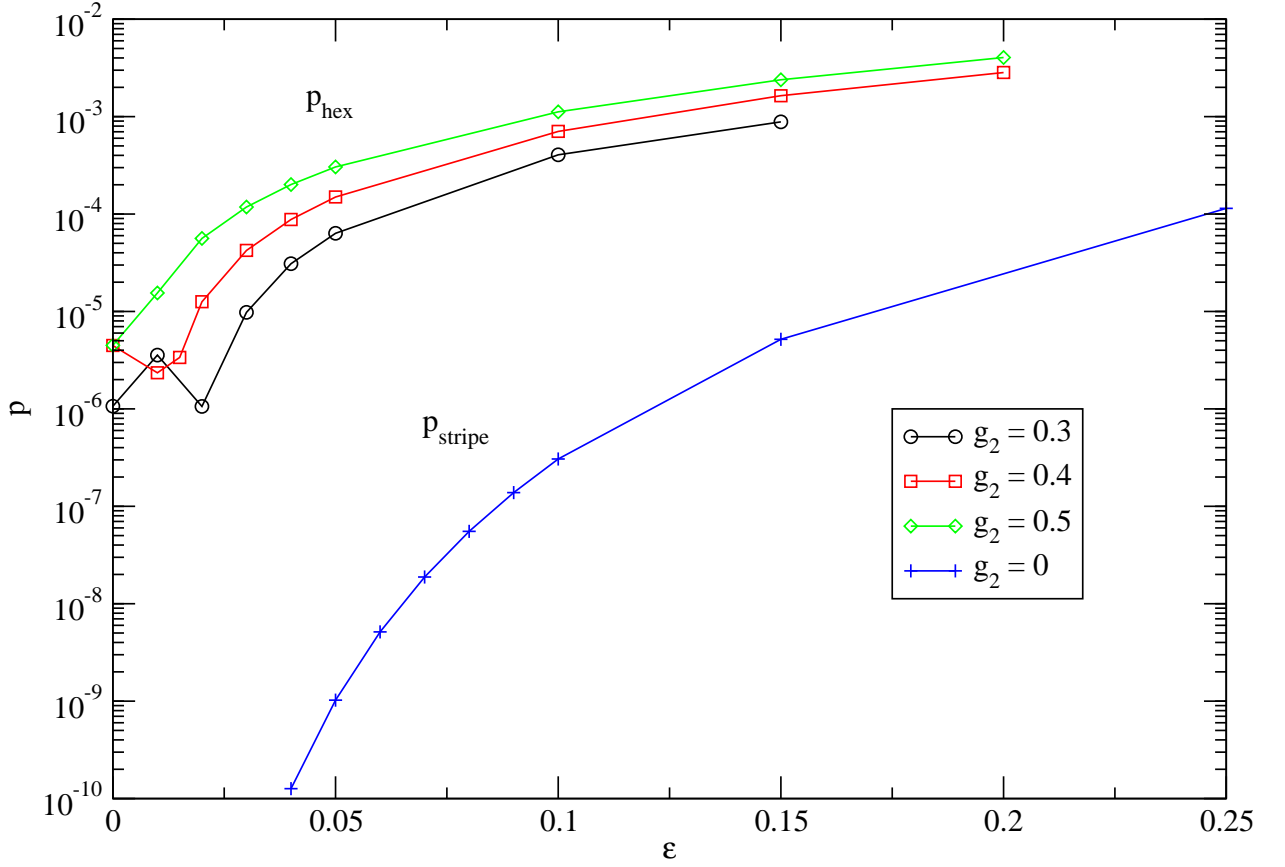


FIG. 2. Values of the pinning force as given by Eq. (6) as a function of ϵ for various values of g_2 ($\theta = \pi/9$ in each case). The result corresponding to a stripe pattern was given in ref. [9], and is shown as a comparison.

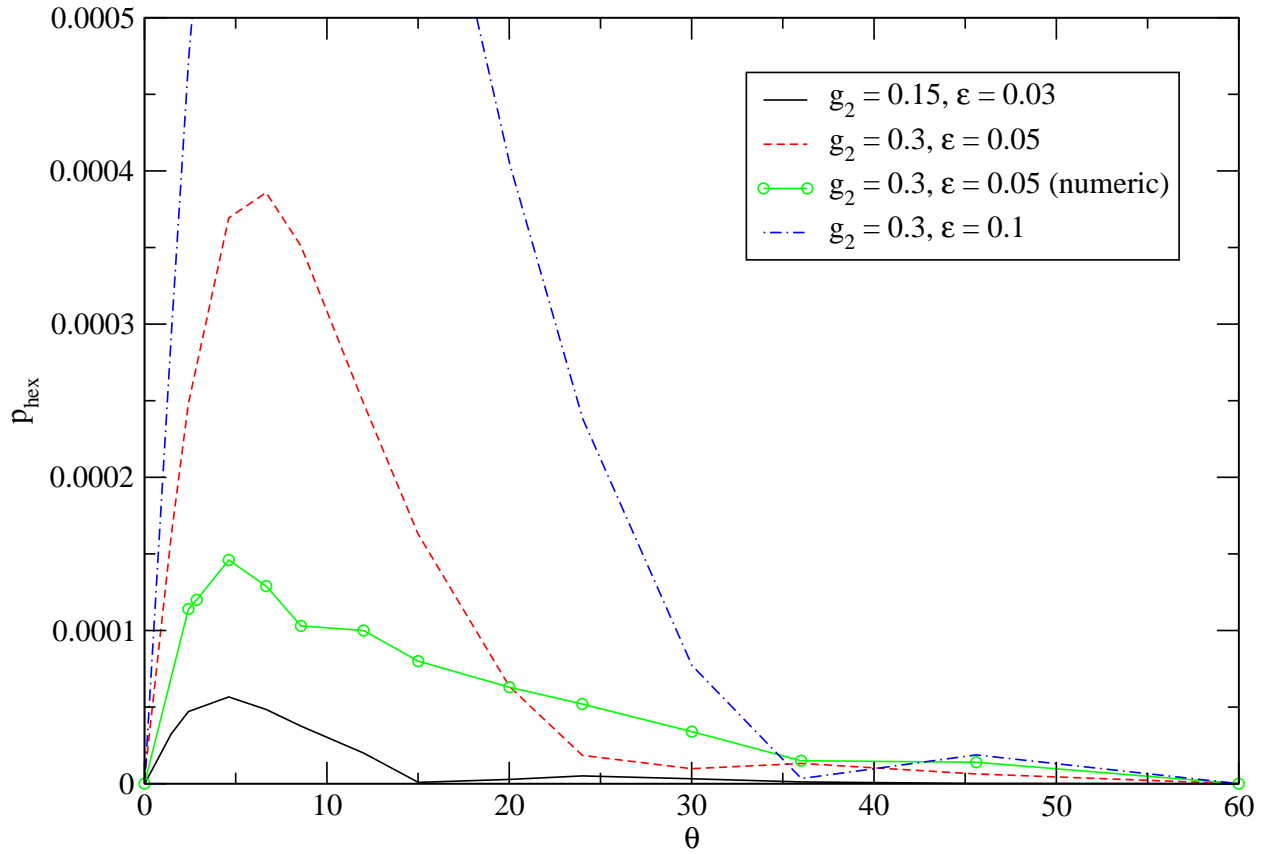


FIG. 3. Angular dependence of the pinning force for various values of g_2 and ϵ obtained analytically with Eq. (6), and numerically for one of the parameter sets.